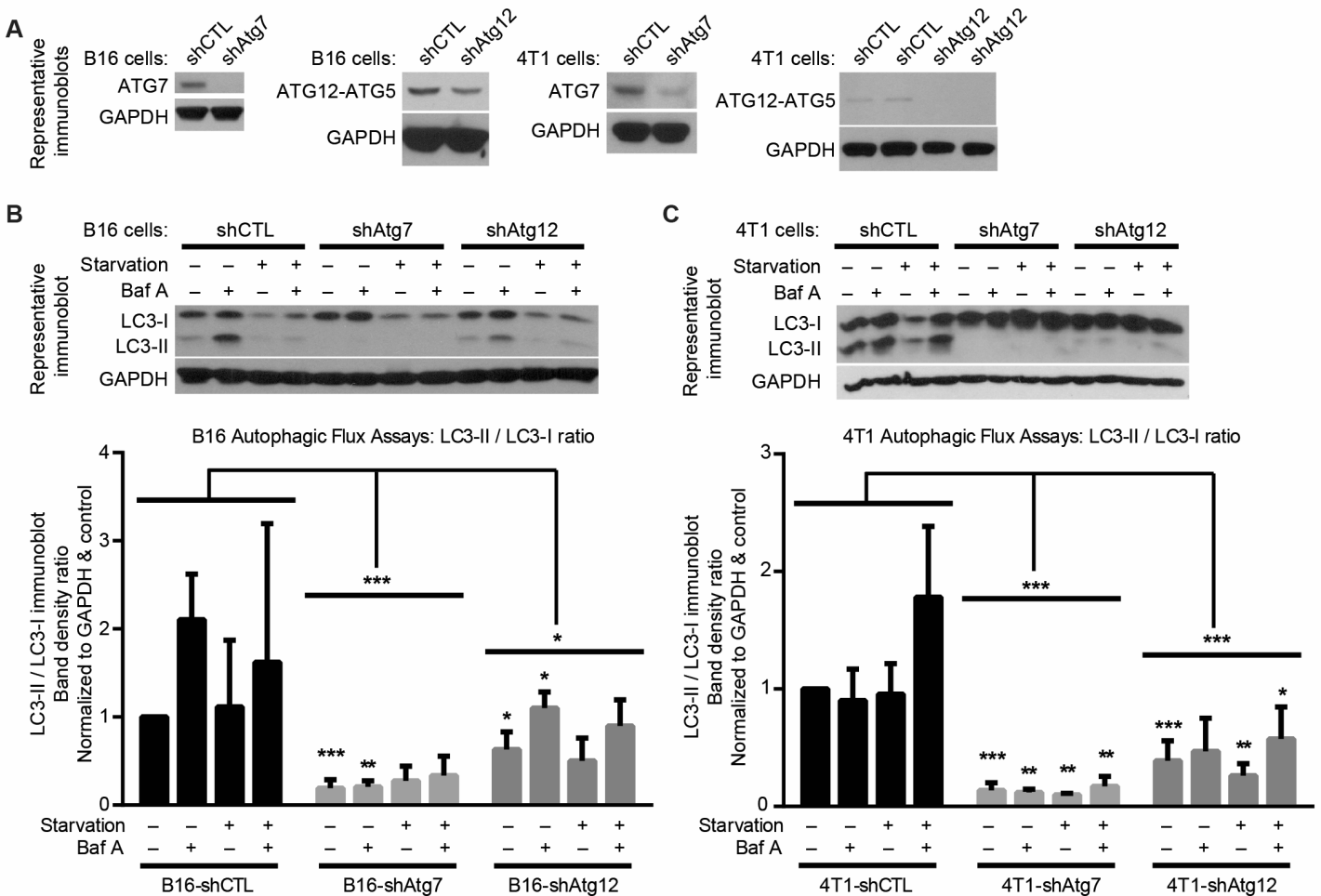


SUPPLEMENTARY MATERIAL TO:

Intact Anti-Tumor Adaptive Immunity Following Autophagy Inhibition and Anti-Malarial Treatment

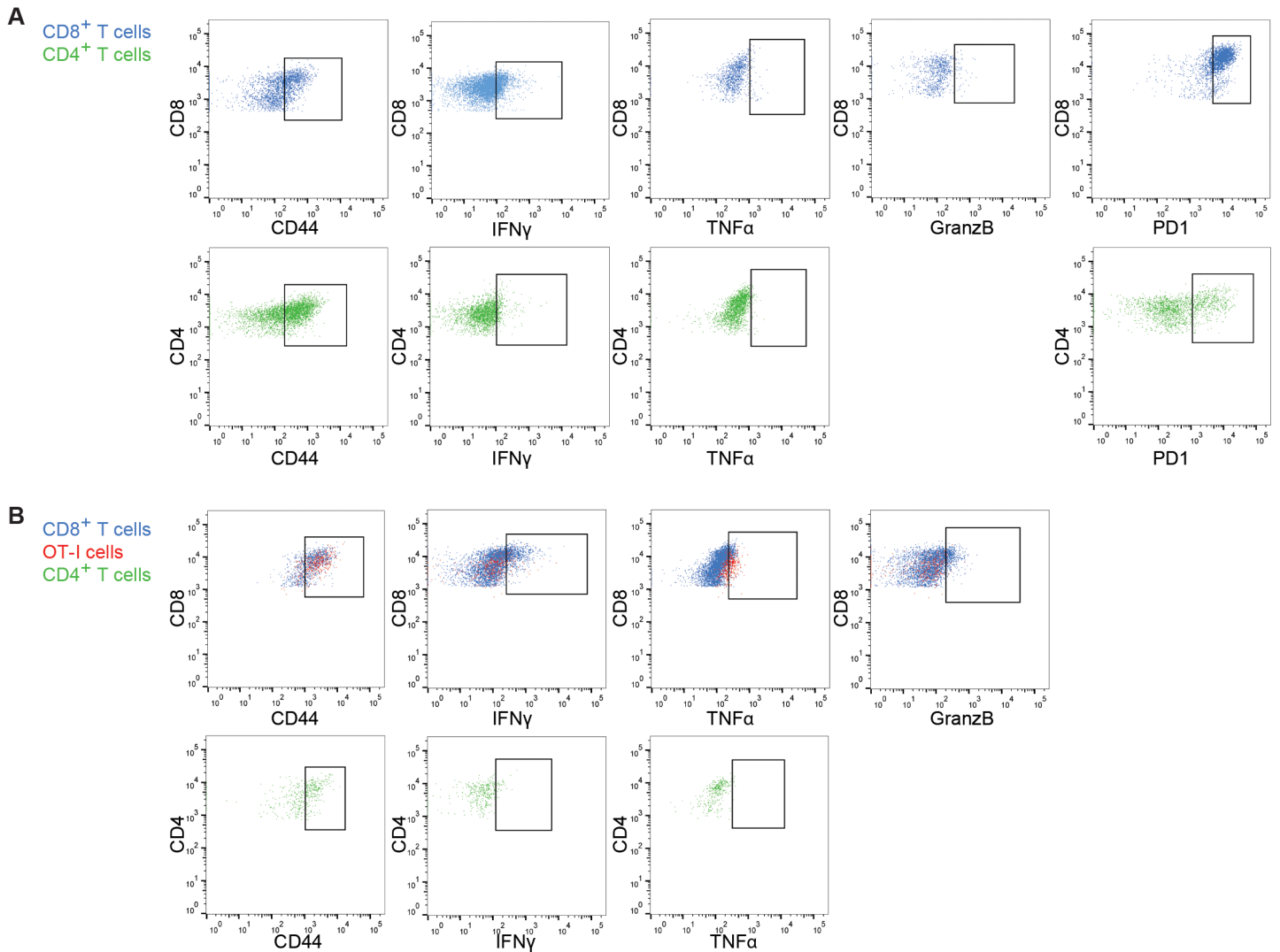
Hanna Starobinets¹, Jordan Ye¹, Miranda Broz¹, Kevin Barry¹, Juliet Goldsmith¹, Timothy Marsh¹, Fanya Rostker¹, Matthew Krummel¹, and Jayanta Debnath¹

Supplementary Figure 1



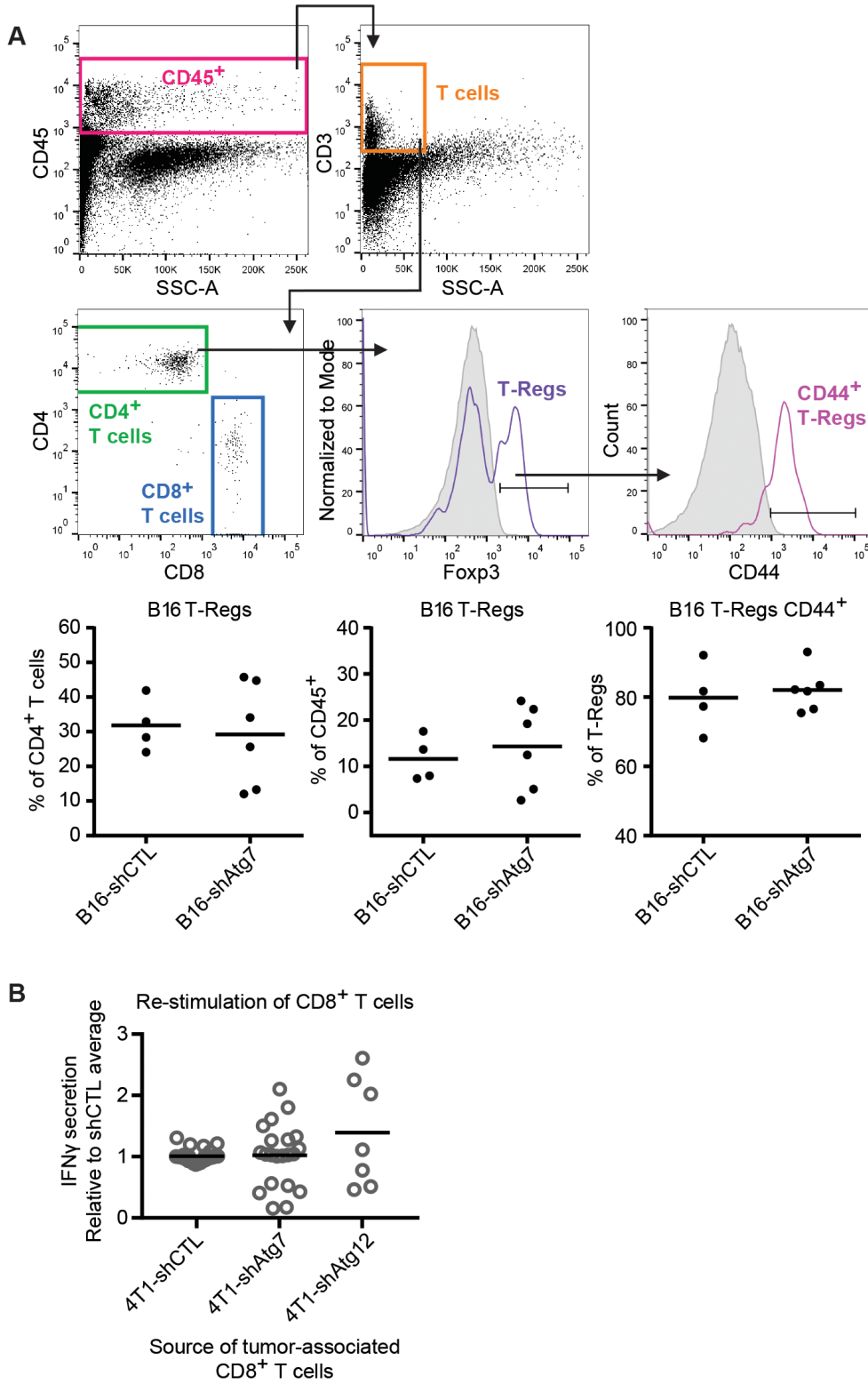
Supplementary Figure 1. Validation of autophagy deficiency in B16 melanoma and 4T1 mammary cancer cells. B16 mouse melanoma and 4T1 mouse mammary cancer cells were infected with lentivirus carrying either non-targeting (shCTL), ATG7 or ATG12 shRNA. (A) ATG7 and ATG12 knockdown was confirmed by immunoblotting. Autophagy flux assays were performed with full medium and starvation conditions, with or without Bafilomycin A (Baf A), with (B) B16 and (C) 4T1 cells. Band density was quantified from α -LC3 immunoblotting of cell lysates from three independent experiments and normalized to GAPDH and control cells grown in full medium without Baf A. Error bars represent standard deviation; * $p < 0.05$, ** $p < 0.01$, *** $p < 0.001$ using unpaired t test.

Supplementary Figure 2



Supplementary Figure 2. Representative dot plots of T cell functional markers. (A) Dot plots corresponding to histograms in Figure 3A. Expression of T cell activation markers (CD44, IFN γ , TNF α , Granzyme B) and immune checkpoint marker PD1 were measured by flow cytometry in CD8⁺ (blue) and CD4⁺ (green) T cell populations. (B) Dot plots correspond to histograms in Figure 4D. Expression of T cell activation markers (CD44, IFN γ , TNF α , Granzyme B) were measured by flow cytometry in endogenous CD8⁺ T cells (blue), adoptively transferred OT-I cells (red), and endogenous CD4⁺ T cells (green).

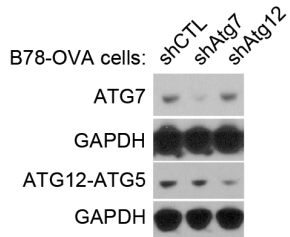
Supplementary Figure 3



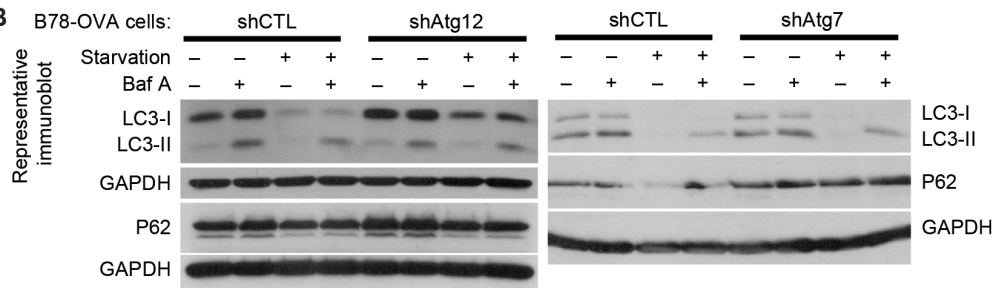
Supplementary Figure 3. T cell suppression and activation potential are unchanged in autophagy-deficient mouse tumors. Subcutaneous B16 tumors were allowed to form for 2 weeks. Tumors were resected and digested enzymatically, and regulatory T (TReg) cell infiltration and functional status were measured by flow cytometry. (A) Top: Representative flow cytometry gating strategy to define TReg cell populations. A live/dead marker was used to define live cells as a subset of singlets. CD45⁺ cells were defined from live cells and T cells were defined as the CD3⁺ SSC-A^{low} fraction of CD45⁺ cells. CD4⁺ and CD8⁺ single-positive T cell populations were subdivided from total T cells, and TRegs were defined as the Foxp3⁺ fraction of CD4⁺ cells. TReg activation was measured by surface CD44 expression. Solid gray plots represent isotype control (for stain of Foxp3) and unstained control (for stain of CD44). Positive staining indicated by gate and defined as that above the unstained or isotype control. Bottom: Each data point represents a distinct tumor from an individual host mouse. Bars represent mean values with two-way ANOVA not significant. (B) CD8⁺ T cells isolated from autophagy-competent and deficient 4T1 tumors are re-stimulated to equivalent activation levels. Orthotopic autophagy-competent (shCTL) and deficient (shAtg7 and Atg12) 4T1 tumors were allowed to form tumors for 2-3 weeks. Tumors were resected and digested enzymatically. CD8⁺ T cells were isolated by either FACS or negative bead selection, and re-stimulated in overnight culture with CD3 and CD28 antibodies. ELISA of conditioned medium from T cell cultures for IFN γ secretion. T cell isolation was performed 5 separate times; each data point represents a distinct conditioned medium sample and bars represent means; unpaired t test not significant.

Supplementary Figure 4

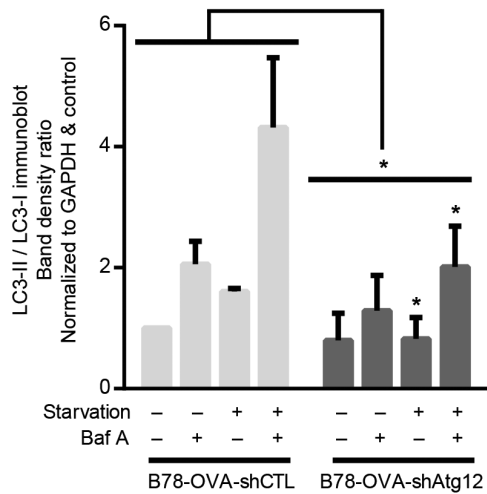
A



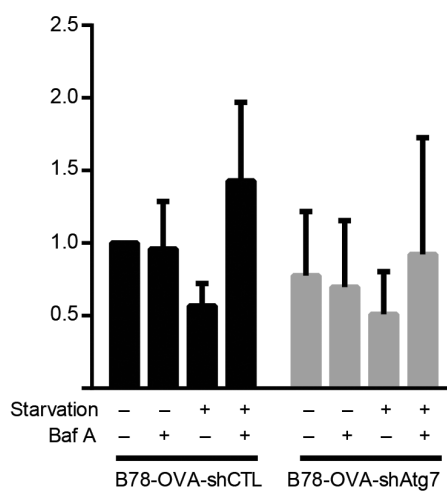
B



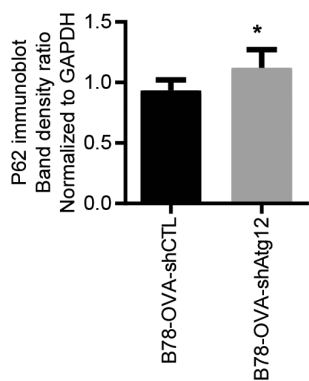
B78-OVA Autophagic Flux Assays: LC3-II / LC3-I ratio



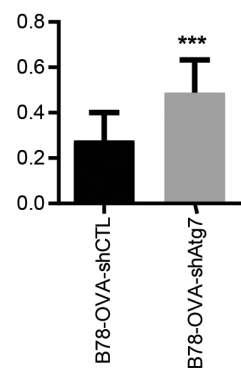
B78-OVA Autophagic Flux Assays: LC3-II / LC3-I ratio



B78-OVA: P62 expression

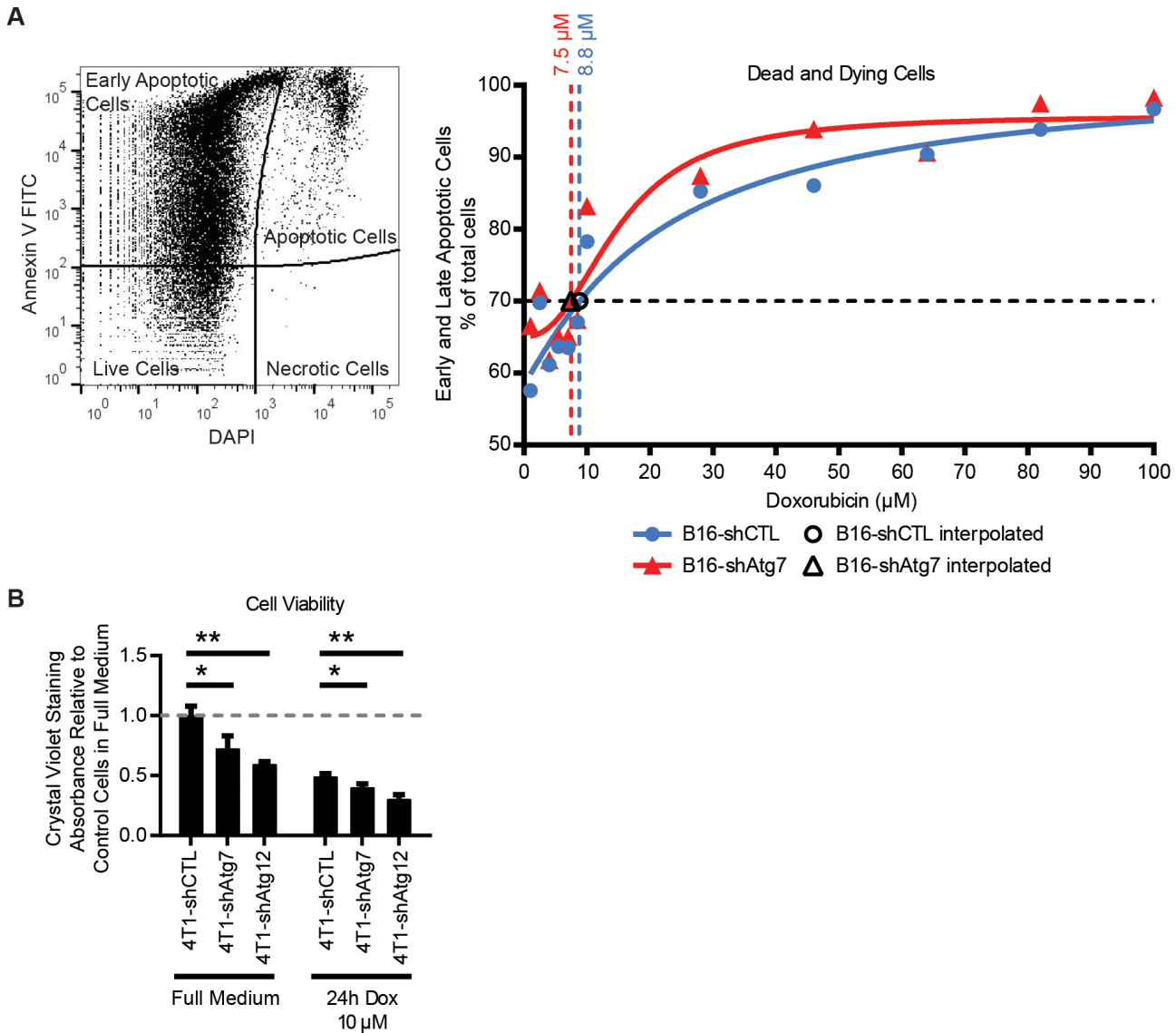


B78-OVA: P62 expression



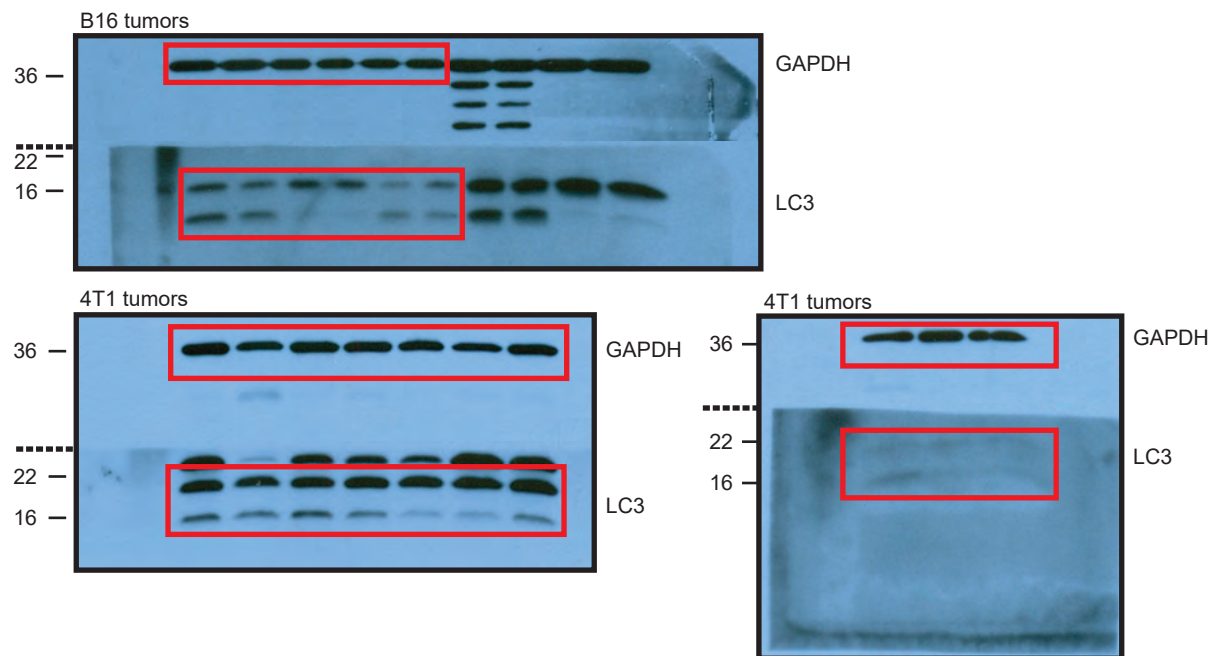
Supplementary Figure 4. Validation of autophagy deficiency in B78-OVA mouse melanoma cells. B78-OVA melanoma cells were infected with lentivirus carrying either non-targeting (shCTL), ATG7, or ATG12 shRNA. (A) ATG7 and ATG12 knockdown were confirmed by immunoblotting. (B) Autophagy flux assays were performed with full medium and starvation conditions, with or without Bafilomycin A (Baf A). Band density was quantified from α -LC3 immunoblotting of cell lysates from three independent experiments and normalized to GAPDH and control cells grown in full medium without Baf A. Error bars represent standard deviation; * $p < 0.05$ using unpaired t test. Band density quantified from P62 immunoblotting of cell lysates from 3 independent experiments and normalized to GAPDH. Error bars represent standard deviation; * $p < 0.05$; *** $p < 0.001$ using unpaired t-test.

Supplementary Figure 5

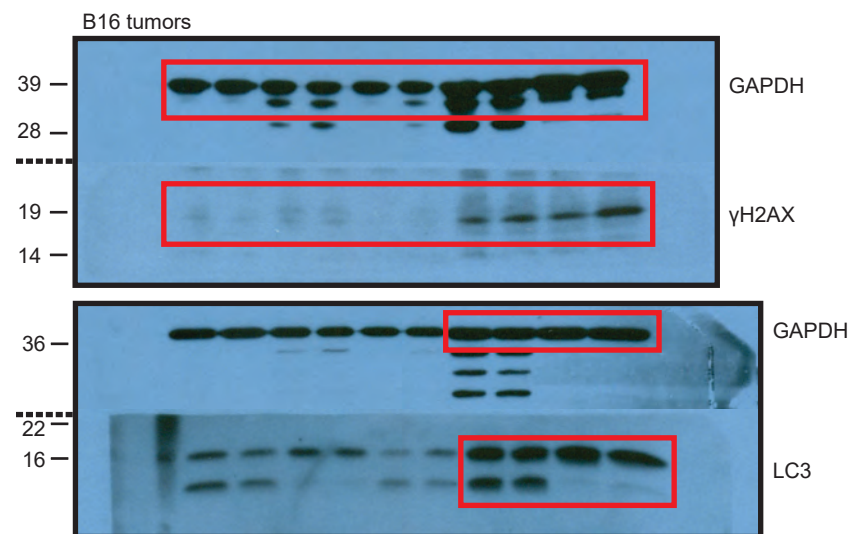


Supplementary Figure 5. Autophagy-deficient cells are more sensitive to doxorubicin treatment. (A) Autophagy-competent (shCTL) and deficient (shAtg7) B16 melanoma cells were cultured for 24 hours with indicated doses of doxorubicin. Floating and adherent cells were collected and stained with an Annexin V kit and DAPI. Representative dot plots of singlet cells analyzed by flow cytometry and divided into quartiles: live cells (Annexin V^{low} DAPI^{low}), early apoptotic cells (Annexin V^{high} DAPI^{low}), apoptotic cells (Annexin V^{high} DAPI^{high}), and necrotic cells (Annexin V^{low} DAPI^{high}). Dead and dying cells were defined as early and late apoptotic populations; dosages that achieved 70% of dead and dying cells were interpolated from the dose-response curve on the right. (B) Autophagy-competent (shCTL) and deficient (shAtg7 or shAtg12) 4T1 mammary carcinoma cells were cultured for 24 hours in full medium or 10 µM Doxorubicin. Cell viability was measured by crystal violet staining (N=3 for each cohort). Error bars represent standard deviation; * p<0.05; ** p<0.01 using unpaired t test.

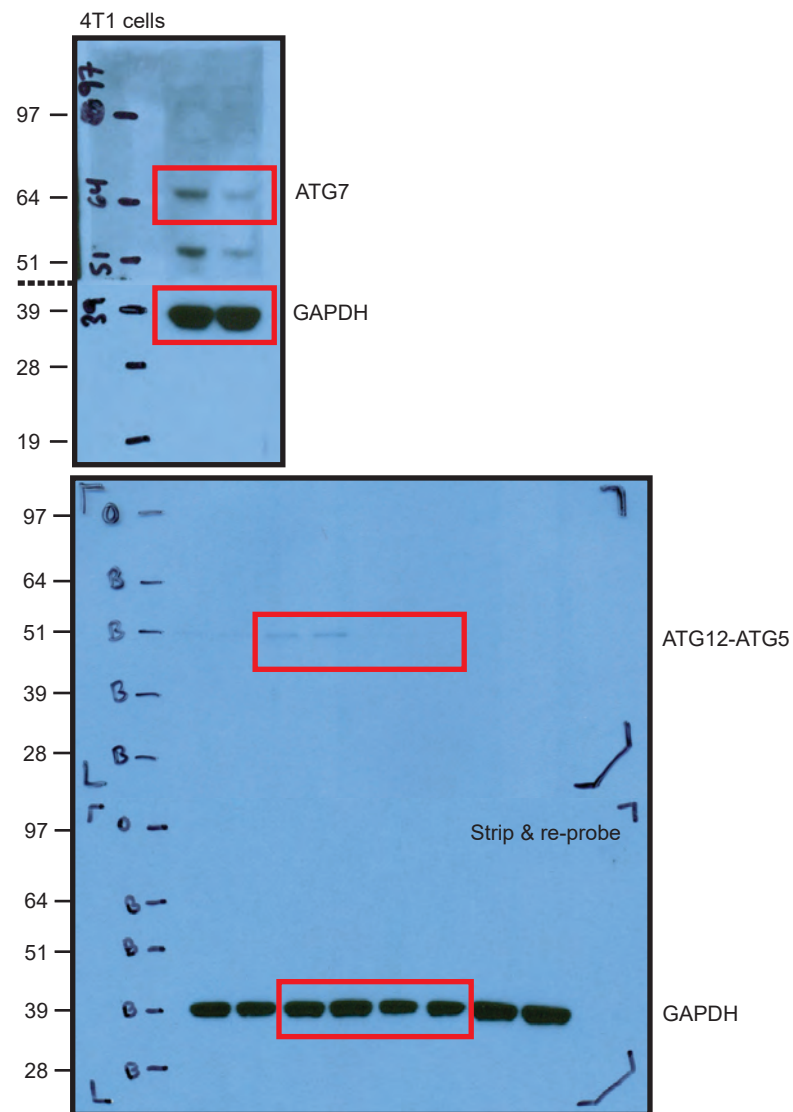
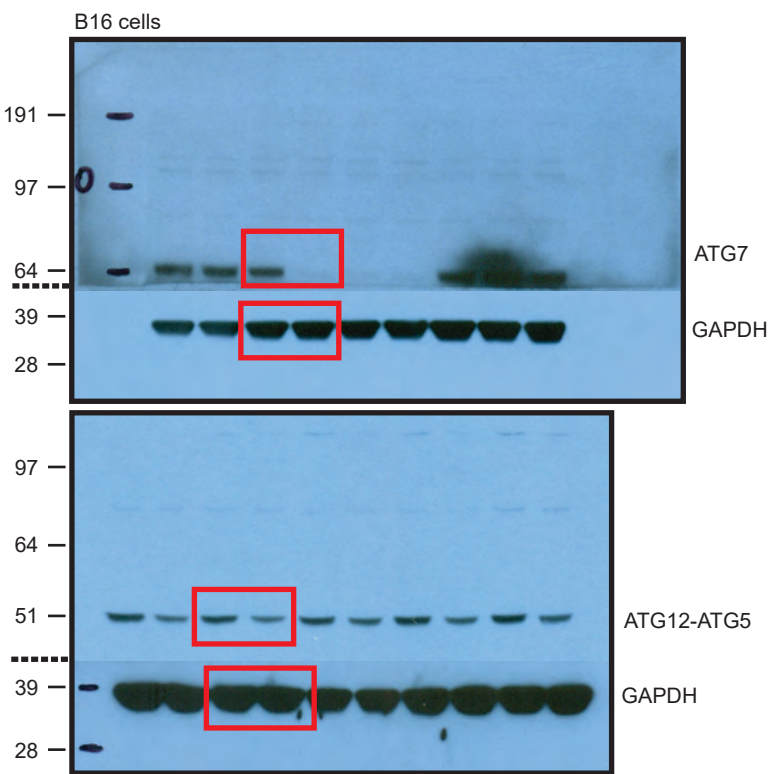
Full unedited gel for Figure 1B



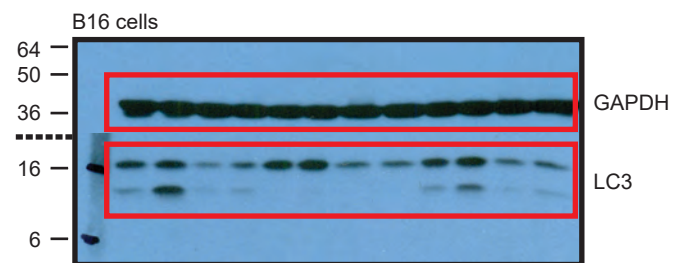
Full unedited gel for Figure 5D



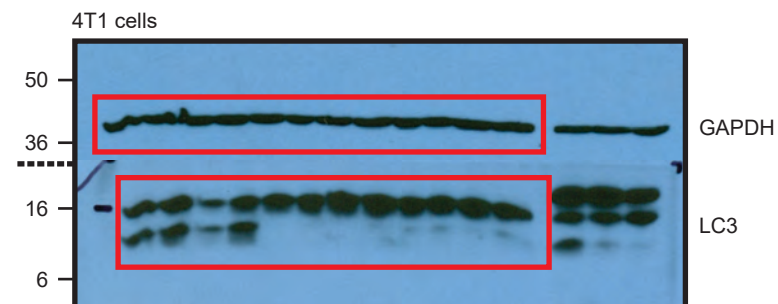
Full unedited gel for Supplementary Figure 1A



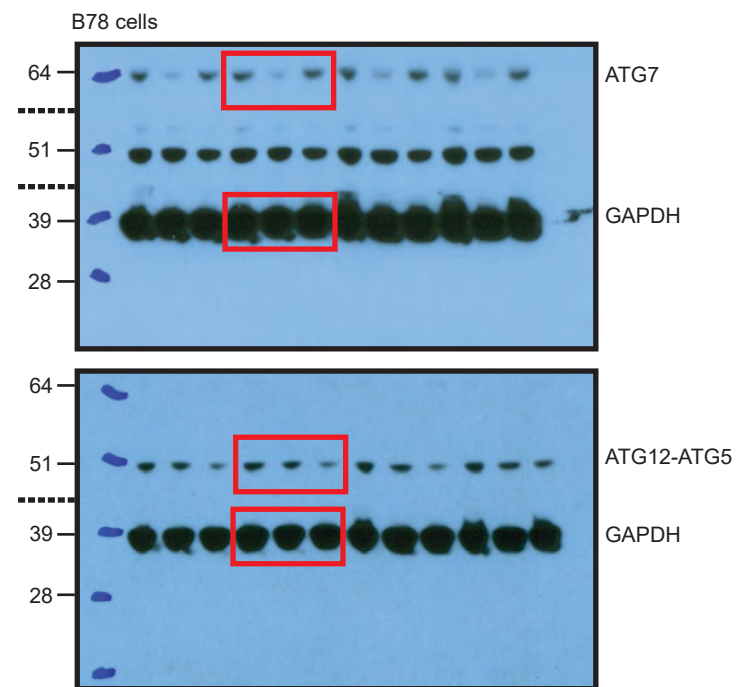
Full unedited gel for Supplementary Figure 1B



Full unedited gel for Supplementary Figure 1C



Full unedited gel for Supplementary Figure 4A



Full unedited gel for Supplementary Figure 4B

